Journal of Alloys and Compounds 505 (2010) 374–378

Contents lists available at ScienceDirect

Journal of Alloys and Compounds

journal homepage: www.elsevier.com/locate/jallcom

Cobalt-coated barium titanate particles: Preparation, characterization and microwave properties

Lixin Ma, Guiqin Wang*, Lidong Liu, Baoyi Li

School of Material Science and Engineering, Dalian University of Technology, Dalian 116024, PR China

ARTICLE INFO

Article history:
Received 12 January 2010
Received in revised form 5 May 2010
Accepted 5 May 2010
Available online 19 June 2010

Keywords:
Barium titanate
Cobalt
Electroless plating
Electromagnetic characteristics
Microwave absorption

ABSTRACT

Barium titanate (BT) particles were coated with Co via electroless plating approach, using hydrazine hydrate as a reducing agent. The BT and Co-coated BT particles were characterized by X-ray diffraction (XRD), transmission electron microscope (TEM), energy dispersive spectroscopy (EDS), vibrating sample magnetometer (VSM) and vector network analyzer. The results showed that Co coating layer with hcp structure was successfully deposited on the surface of the BT. The magnetic properties of the Co-coated BT were significantly improved. The complex permittivity and permeability of the Co-coated BT were higher than those of BT. Co-coated BT with much thinner absorber thickness achieved better microwave absorption properties in comparison with uncoated BT. The microwave enhancement absorption of Co-coated BT was related to the enhanced dielectric and magnetic losses.

1. Introduction

With the dramatic development of electronic systems and communication technology, electromagnetic (EM) waves have been extensively used in both military and civil field. However, many adverse effects such as electromagnetic interference (EMI), electromagnetic compatibility (EMC), EM information leakage, and potential health hazards of EM radiation have emerged along with the increasing use of EM waves [1–4]. Therefore, the development of EM wave absorbers is strongly demanded. Much effort currently has been directed towards exploiting new EM wave absorbers with properties such as strong absorption, wide frequency range, lightweight, thinness, and environmental resistivity [5–8]. It is believed that the microwave absorption performances are associated with the complex permittivity ($\varepsilon_r = \varepsilon' - j\varepsilon''$), the complex permeability ($\mu_r = \mu' - j\mu''$), the EM impedance match, and the microstructure of the absorber [9].

Recently, some researches have been focused on barium titanate ($BaTiO_3$ or BT), which can be used as microwave absorber motivated by its good permittivity properties, ease of preparation, as well as low cost [10–14]. Nevertheless, the complex permeability of BT is low, which limits its microwave absorbing characteristics. Therefore, in order to optimize the microwave absorption performances, it is necessary to modify the magnetic characteristics of BT. Electroless plating technique, which has seen considerable use in preparing metallic coatings on fine substrates [15–17], provides a possible way to realize the modification of BT. The reducing agent most commonly used in electroless plating is sodium hypophosphite. However, the electroless coating obtained using sodium hypophosphite contains nonmagnetic element P which could weaken the magnetic properties of the product. Typically, the coating containing P in excess of 8 wt.% is nonmagnetic [18,19]. The formation of pure metal coating can be realized by using hydrazine hydrate as a reducing agent. To the best of our knowledge, no reports concerning electroless plating magnetic metal on BT with hydrazine hydrate as reducing agent have previously been published.

In this paper, Co-coated BT particles were prepared by an electroless plating technique using hydrazine hydrate as a reducing agent. The structure, morphology and magnetic properties of the Co-coated BT particles were studied. The microwave electromagnetic and absorption properties were also investigated.

2. Experimental

2.1. Preparation of $BaTiO_3$ powders

BT powders were prepared by sol–gel technique. The synthesis procedure is described as follows. 4.925 g barium carbonate was first dissolved in the solution of glacial acetic acid. Then, the mixed solution of tetrabutyl titanate and 20 mL anhydrous ethanol was added into the above solution. The molar ratio of Ba and Ti ions was controlled as 1:1. The final solution was stirred vigorously for 40 min, gelling at 60 °C and the xerogels were obtained at 80 °C. BT powders were obtained via heat treatment at 950 °C for 3 h.

* Corresponding author. Tel.: +86 411 84708446; fax: +86 411 84716983.
E-mail address: wanggq@dlut.edu.cn (G. Wang).

0925-8388/$ – see front matter © 2010 Elsevier B.V. All rights reserved.
doi:10.1016/j.jallcom.2010.05.184

Table 1
The composition of the electroless cobalt bath.

Ingredient	Molecular formula	Content
Cobalt sulfate, heptahydrate	$CoSO_4{\cdot}7H_2O$	0.1 mol/L
Hydrazine hydrate	$N_2H_4{\cdot}H_2O$	60 mL/L
Potassium sodium tartrate	$C_4H_4KNaO_6{\cdot}4H_2O$	50 g/L
Thiourea	CH_4N_2S	0.5 mg/L

2.2. Pre-treatment of $BaTiO_3$ powders

The as-prepared BT powders were pre-treated to produce catalytic activity through the following procedure. First, the powders were surface coarsed at the solution of NH_4F (2 g/L) with ultrasonic vibration for 30 min. And then, the coarsened powders were sensitized and activated by the solution of $PdCl_2$ (0.5 g/L), $SnCl_2{\cdot}2H_2O$ (25 g/L), HCl (60 mL/L) and NaCl (140 g/L) using ultrasonic vibration for 60 min. Finally, the powders were separated from solution through centrifugation, washed with deionized water and dried at 60 °C.

2.3. Electroless deposition cobalt process

The pre-treatment BT powders were dipped in an electroless plating bath with composition given in Table 1. The chemical equation of the reduction is described below:

$$2Co^{2+} + N_2H_4 + 4OH^- \rightarrow 2Co + N_2\uparrow + 4H_2O \quad (1)$$

The bath solution with pH adjusted by sodium hydroxide to 11.0 was maintained at a constant temperature of 85 °C. The electroless plating was carried out for 60 min under stirring. After plating, the powders were separated from solution by magnetic separation and rinsed with deionized water several times, followed by drying in a vacuum oven at 60 °C.

2.4. Characterization

X-ray diffraction (XRD; XRD-6000, SHIMADZU) was used to identify phase structure at a scan rate of 4°/min with Cu Kα radiation (λ = 0.15406 nm, 40.0 kV, 30.0 mA) in the 2θ range from 20° to 85°. The morphology was observed via transmission electron microscope (TEM; JEM-100CXII, FEI). Energy dispersive spectroscopy (EDS) analysis was performed to determine the chemical composition of the plated powders. The static magnetic properties were examined at room temperature by means of a vibrating sample magnetometer (VSM; JDM-13). The EM parameters (complex permeability and permittivity) were measured using a vector network analyzer (HP 8720ES) in the frequency range of 2–18 GHz. The samples used for EM parameters measurement were prepared by dispersing powders into paraffin wax with mass fraction of 70%, and then pressing the mixtures into toroidal-shaped compact. According to the transmission line theory, the reflection loss (RL) curves were calculated using measured EM parameters at a given frequency and absorber thickness.

3. Results and discussion

3.1. Structure and morphology analysis

Typical XRD patterns of uncoated BT and Co-coated BT are presented in Fig. 1(a) and (b), respectively. From Fig. 1(a), all the peaks can be indexed as perovskite $BaTiO_3$ (JCPDS # 05-0626) and no impurity phases are detected. The diffraction pattern of the Co-coated BT in Fig. 1(b) exhibits clear cobalt peaks in addition to strong $BaTiO_3$ peaks. The peaks appearing at around 41.5°, 44.4°, 47.5° and 75.8° correspond to (1 0 0), (0 0 2), (1 0 1), (1 1 0) crystal planes of the hcp Co (JCPDS # 05-0727). It is worth noting that the relative intensity of the peaks corresponding to the (0 0 2)/(1 0 1), (0 0 2)/(1 1 0) planes are higher than the standard values in JCPDS card, indicating that the deposited Co may have preferential crystal growth [20]. The cobalt phase possesses a crystalline rather than an amorphous structure which was found in Co–P electroless plating coating [21]. This indicates that a single element is more likely

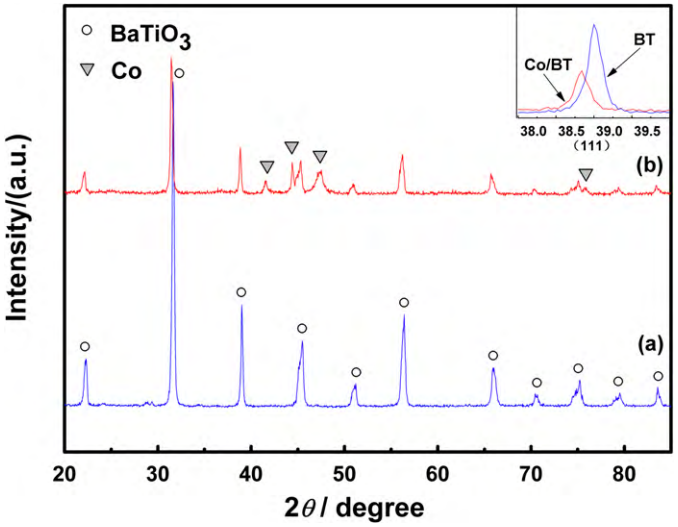

Fig. 1. XRD patterns of (a) BT and (b) Co-coated BT.

to form a crystalline structure than a multiple element system. Additionally, no discernible third phases can be detected from the pattern, which indicates that no reaction has taken place between Co and $BaTiO_3$ in the Co-coated BT. The upper right inset shows the (1 1 1) peaks of the uncoated BT and Co-coated BT, respectively. Clearly noted is that the (1 1 1) peak is shifted to a lower angle, when the particles are coated with Co. The shift of the peak position to a low angle indicates that the tensile stress is caused by the cobalt coating layer [22].

The average particle size of BT is estimated from the line broadening of corresponding X-ray diffraction peaks using the Scherrer formula [23]:

$$D = \frac{0.9\lambda}{\beta \cos\theta} \quad (2)$$

where D is the particle size (nm), λ the wavelength of the X-ray radiation, β the line width at half maximum height, and θ the diffracting angle. The average particle size of the prepared BT is calculated to be 79 nm.

The lattice constants, crystal cell volume and density of BT before and after plating are listed in Table 2, where the lattice constants are analyzed by Jade5 software and the density can be obtained according to the following Eq. (3):

$$\rho = \frac{nM}{N_A V} \quad (3)$$

ρ is the density, n the number of molecules contained in one crystal cell, M the molecular weight, N_A Avogadro constant ($N_A = 6.02 \times 10^{23}$), and V the crystal cell volume.

As shown in Table 2, it is clear that the tetragonality (c/a) of BT is enhanced after electroless cobalt plating. The reasons can be concluded as follows. The coating layer exerts a tensile stress on the BT particles. On the other hand, the conductive coating can reduce depolarization energy of BT particles and, thereby, promotes the polar tetragonal phase [22]. The lattice constants and crystal cell volume of the BT particles are increased after coating due to the effect of tensile stress on the BT particles, and the density of BT is decreased by cobalt coating layer.

Table 2
The lattice constants, crystal cell volume and density of BT before and after plating.

Sample	a (Å)	c (Å)	c/a	V (Å^3)	ρ (g cm^{-3})
Uncoated BT	3.9933	4.0164	1.0058	64.05	6.0469
Coated BT	3.9992	4.0369	1.0094	64.56	5.9985

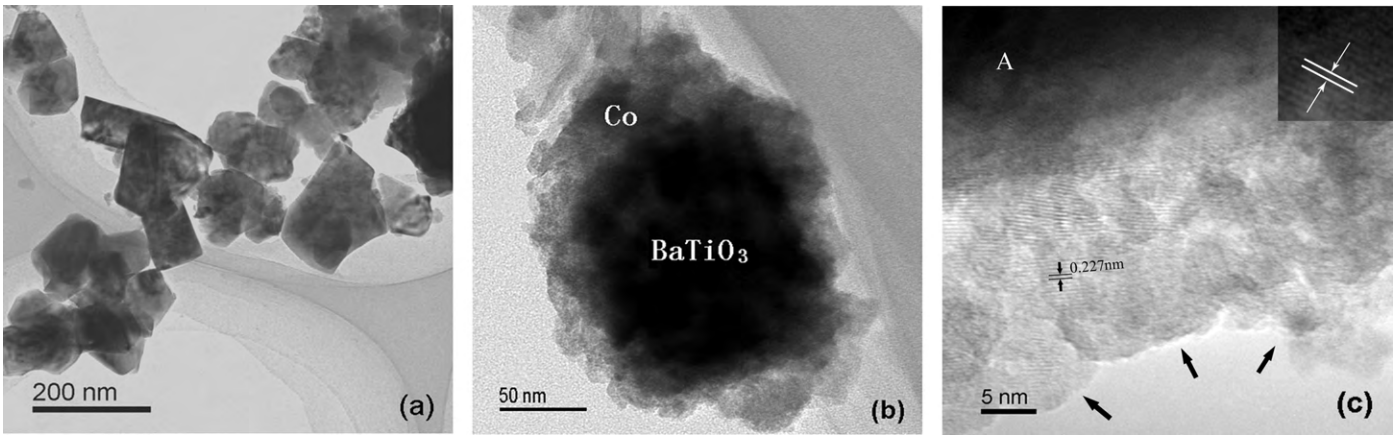

Fig. 2. TEM images of (a) uncoated BT, (b) Co-coated BT and (c) HRTEM image of Co-coated BT showing the crystal nanograins of Co.

A TEM micrograph of uncoated BT is displayed in Fig. 2(a). It is observed that the BT particles are irregular in shape with dimensions in the range 60–150 nm. Fig. 2(b) shows a representative TEM micrograph of Co-coated BT, from which it can be seen that the particle has a core/shell structure with a clearly distinguishable interface, containing BT nanoparticle as core and Co as shell. The outer cobalt shell is mainly uniform around 20 nm in thickness and BT nanoparticle is encapsulated completely. The HRTEM image, Fig. 2(c), shows that the deposited cobalt layer is composed of crystal nanoparticles (as indicated by arrows). The enlarged observation (inset in Fig. 2(c)) on the core region A shows the lattice fringes with a d-spacing of 0.285 nm, corresponding to the (1 0 1) plane of BT. The lattice spacing of the selected area in shell region is about 0.227 nm, which can be indexed to the (1 0 0) plane of hcp Co.

EDX analysis of Co-coated BT is presented in Fig. 3. As shown in Fig. 3, Co, Ba, Ti and O elements are all found, which further confirms the presence of cobalt in the Co-coated BT particles. Therefore, it is believed that the Co layer was deposited successfully on the surface of the BT particles.

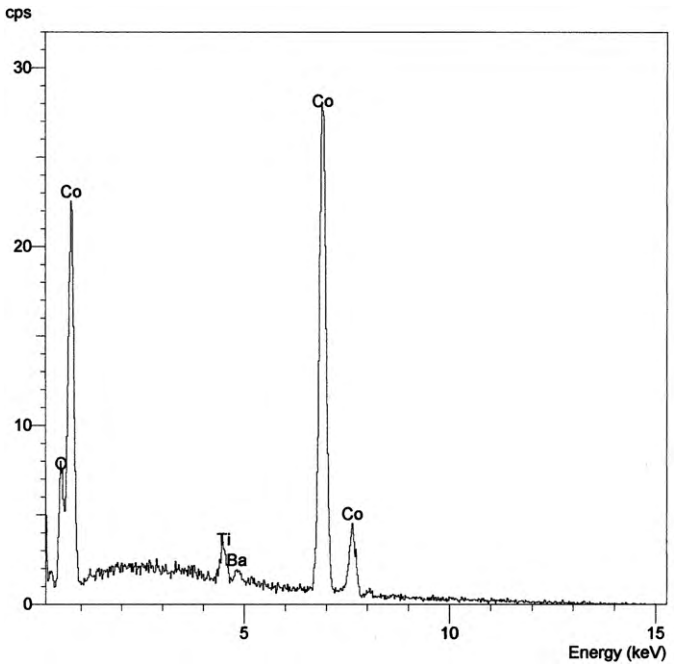

Fig. 3. EDX analysis of Co-coated BT.

3.2. Magnetic properties

Fig. 4 shows the magnetization curves for uncoated BT and Co-coated BT measured at room temperature. It can be seen that the uncoated powders show a paramagnetic behavior, while the plated powders present a ferromagnetic behavior with a saturation magnetization (Ms) of 40.98 emu/g, a remnant magnetization (Mr) of 6.22 emu/g, and a coercivity (Hc) of 373 Oe. The Ms of the Co coating is much higher than that of amorphous Co–B electroless coating [24]. It is well known that magnetic characteristics of crystalline materials are significantly larger than those of amorphous materials. Clearly, the Co-coated BT powders exhibit much enhanced magnetic properties compared with the uncoated BT. It is supposed that the improved magnetic performances of the Co-coated BT could increase the magnetic loss in microwave absorption.

3.3. Microwave electromagnetic properties

The complex permittivities of BT and Co-coated BT in the frequency range of 2–18 GHz are shown in Fig. 5. As seen from Fig. 5, the curves of complex permittivity for the BT and Co-coated BT exhibit the same trend, i.e., the values of ε' remain almost constant at lower frequency and then display slight fluctuation in the higher frequency range, while the values of ε'' increase slightly with

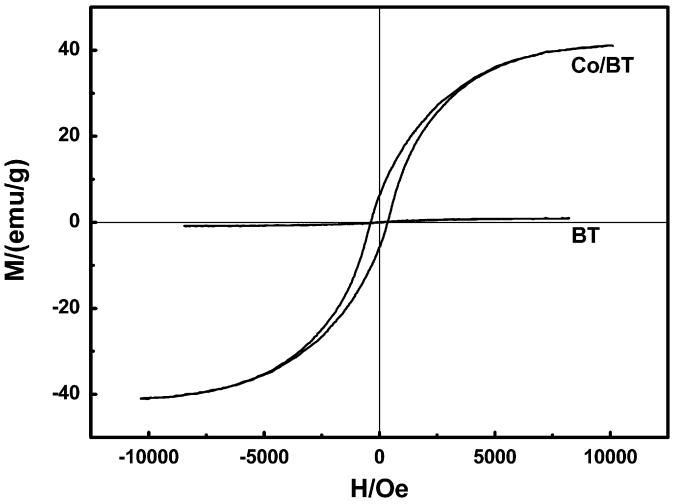

Fig. 4. Magnetization curves of BT and Co-coated BT measured at room temperature.

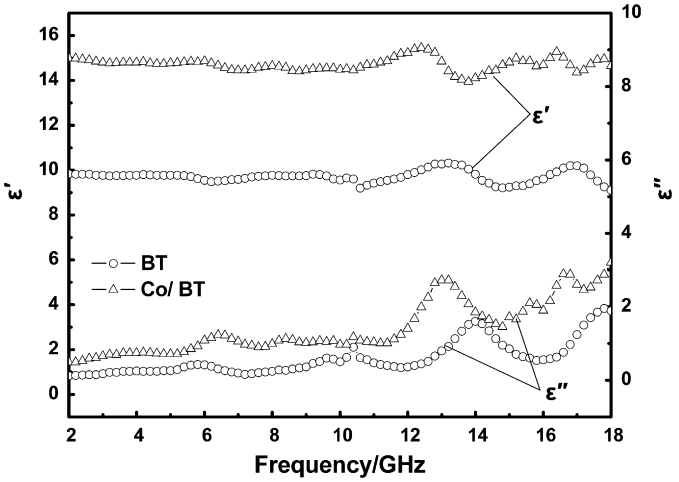

Fig. 5. The complex permittivity for BT and Co-coated BT.

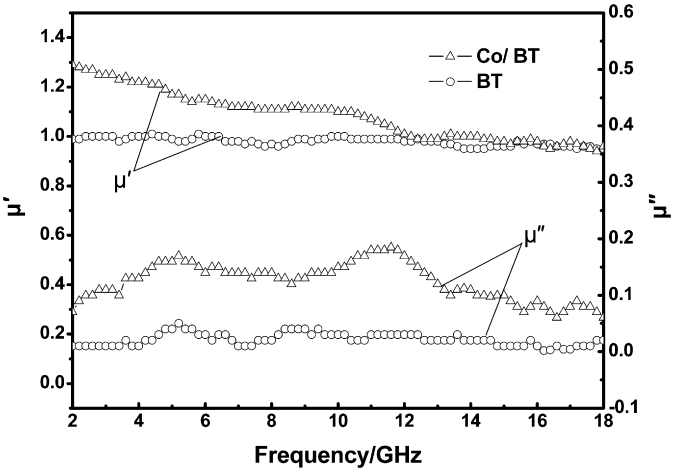

Fig. 6. The complex permeability for BT and Co-coated BT.

frequency. Moreover, ε'' curves present a resonance peak. This is thought to be due to the dielectric relaxation behavior in BT. The resonance peak of the Co-coated BT moves slightly toward lower frequency as compared to the BT, which may be attributed to the effect of tensile stress on BT particles [25]. Apparently, both ε' and ε'' values of the Co-coated BT are higher than those of the BT in the whole frequency range. The higher value of ε' for the Co-coated BT is ascribed to interfacial polarization between adjacent conductive particles separated by insulating paraffin matrix [26]. According to the relation $\varepsilon'' = \sigma/2\pi f\varepsilon_0$ [27], where σ is the electrical conductivity, the ε'' value of the Co-coated BT should be higher than that of the BT. This estimation is in good agreement with the measured result. The increased ε'' indicates higher dielectric loss in the Co-coated BT.

BT is a dielectric material, the dominant dipolar polarization, spontaneous polarization and the associated relaxation phenomena constitute the loss mechanisms. The tetragonality of BT particle is closely related to the intensity of spontaneous polarization. The larger the tetragonality, the stronger the spontaneous polarization. Therefore, stronger spontaneous polarization occurs in the Co-coated BT particles. The relaxation associated with the interfacial polarization will also lead to a loss mechanism and the dielectric relaxation behavior becomes more complicated, for the Co-coated BT particles. In addition, the conductive composite particles may form certain conductive network, leading to the attenuation of incident electromagnetic waves.

Fig. 6 shows the complex permeabilities of BT and Co-coated BT in the frequency range from 2 to 18 GHz. For the BT, the real part μ' and imaginary part μ'' are observed to keep nearly invariable with increasing frequency. And the complex permeability is low. For the Co-coated BT, the μ' exhibits a decline trend over the range of 2–18 GHz with values from 1.29 to 0.96. This is favorable for microwave surface impedance match [28]. The μ'' presents a broad resonance peak around 11.4 GHz. The dimensions of Co nanoparticles are smaller than the skin depth, so the effect of eddy current on the permeability can be neglected. The resonance peak may be related to the exchange resonance modes. For nanoparticles, the exchange contributions become important and will give rise to exchange resonance modes [29]. The broad resonance peak could be attributed to the larger damping parameter [30]. Consistent with expectation, Co coating layer increases complex permeability. Moreover, it can be clearly observed that μ'' value of the Co-coated BT is much higher than that of the BT, which is ascribed to the high magnetization of Co coating layer. The enhanced μ'' indicates that the magnetic loss of the Co-coated BT is increased.

3.4. Microwave absorption properties

In order to further reveal the microwave absorption performances, the RL of electromagnetic radiation was calculated at a given frequency and absorber thickness according to the following formulas:

$$RL(dB) = 20 \log \left| \frac{Z_{in} - Z_0}{Z_{in} + Z_0} \right| \quad (4)$$

$$Z_{in} = \sqrt{\frac{\mu_0 \mu}{\varepsilon_0 \varepsilon}} \tanh(j2\pi f d \sqrt{\mu\mu_0 \varepsilon\varepsilon_0}) \quad (5)$$

where Z_{in} is the input impedance of absorber, Z_0 is the impedance of free space (376.7 Ω), μ_0 and ε_0 are the permeability and permittivity of free space, μ and ε are the complex permeability and permittivity, respectively, f is the frequency of the EM wave, and d is the thickness of absorber.

Fig. 7 shows the frequency dependence of the calculated reflection loss for BT and Co-coated BT. Obviously, when the thickness layer is 1.5 mm, the RL for BT is relatively poor, with a minimum RL value of −11.4 dB at 17.8 GHz. The optimal RL of BT reaches −20.7 dB at 14.4 GHz (f_m) with a matching thickness (d_m) of 5.2 mm and the RL values less than −10 dB are achieved in the 13.1–15.1 GHz range. In comparison, an optimal RL value of −26.12 dB for Co-coated BT

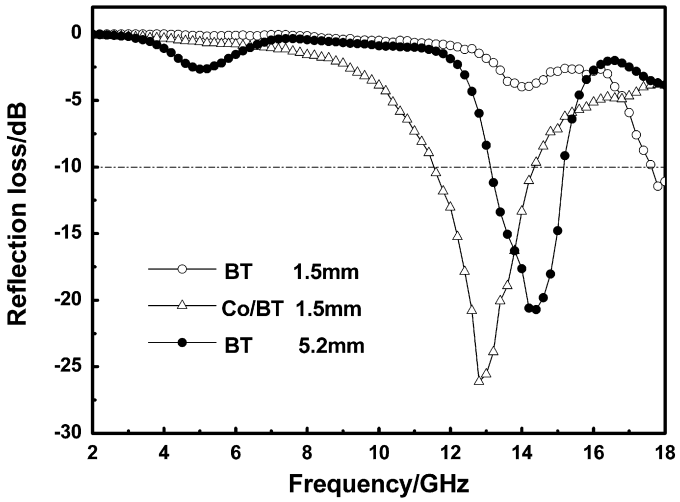

Fig. 7. Reflection loss as a function of frequency for the BT and Co-coated BT.

is obtained at 12.8 GHz (f_m) with a matching thickness of 1.5 mm and the RL values is below −10 dB at 11.5–14.3 GHz. It is worth noting that Co-coated BT has the broader bandwidth (RL < −10 dB) and the thinner absorber matching thickness (1.5 mm). The microwave absorption performances of the Co-coated BT are better than that of the BT. For pure BT, the dielectric loss mainly contributes to the energy loss of EM wave, while for pure Co particles, the magnetic loss becomes dominant over the dielectric loss. However, Co-coated BT effectively combines dielectric and magnetic losses by the special core/shell microstructure, exhibiting good microwave absorption properties.

4. Conclusions

The BT powders were prepared by sol–gel technique and successfully coated with Co layer via electroless plating method by using hydrazine hydrate as a reducing agent. It is found that the deposited layer composed of nanoparticles is pure Co with hcp structure. After coating with a layer of Co, the tetragonality, lattice constants and crystal cell volume of the BT are increased and the density is reduced. Moreover, the complex permittivity and permeability increase, and the dielectric and magnetic losses are enhanced, especially the increase of the magnetic loss is evident. Compared with BT, Co-coated BT attains better microwave absorption performances with much thinner thickness. The optimal reflection loss reaches −26.12 dB at 12.8 GHz with a matching thickness of 1.5 mm and the bandwidth with a reflection loss less than −10 dB is 2.8 GHz. The improved microwave absorption of Co-coated BT is thought to be related to the enhanced dielectric and magnetic losses.

References

[1] K. Sakai, N. Asano, Y. Wada, S. Yoshikado, J. Eur. Ceram. Soc. 30 (2010) 347–353.
[2] Z.B. Li, Y.D. Deng, B. Shen, L. Liu, W.B. Hu, J. Alloys Compd. 491 (2010) 406–410.
[3] Y.N. Kazantsev, A.V. Lopatin, N.E. Kazantseva, A.D. Shatrov, V.P. Mal'tsev, J. Vil˘cáková, P. Sáha, IEEE Trans. Antennas Propag. 58 (2010) 1227–1235.
[4] Y.P. Duan, S.H. Liu, H.T. Guan, Sci. Technol. Adv. Mater. 6 (2005) 513–518.
[5] J. Zeng, J.C. Xu, J. Alloys Compd. 493 (2010) L39–L41.
[6] S.B. Ni, X.H. Wang, G. Zhou, F. Yang, J.M. Wang, D.Y. He, J. Alloys Compd. 489 (2010) 252–256.
[7] X.J. Wei, J.T. Jiang, L. Zhen, Y.X. Gong, W.Z. Shao, C.Y. Xu, Mater. Lett. 64 (2010) 57–60.
[8] Y. Yang, C.L. Xu, Y.X. Xia, T. Wang, F.S. Li, J. Alloys Compd. 493 (2010) 549–552.
[9] X.F. Zhang, X.L. Dong, H. Huang, Y.Y. Liu, W.N. Wang, X.G. Zhu, B. Lv, J.P. Lei, C.G. Lee, Appl. Phys. Lett. 89 (2006) 053115.
[10] C.C. Yang, Y.J. Gung, W.C. Hung, T.H. Ting, K.H. Wu, Compos. Sci. Technol. 70 (2010) 466–471.
[11] G.Q. Wang, X.D. Chen, Y.P. Duan, S.H. Liu, J. Alloys Compd. 454 (2008) 340–346.
[12] Y.K. Liu, Y.J. Feng, X.W. Wu, X.G. Han, J. Alloys Compd. 472 (2009) 441–445.
[13] L.N. Jing, G.Q. Wang, Y.P. Duan, Y.Z. Jiang, J. Alloys Compd. 475 (2009) 862–868.
[14] C. Wang, X.J. Han, P. Xua, X.H. Wang, X.A. Li, H.T. Zhao, J. Alloys Compd. 476 (2009) 560–565.
[15] J.W. Yi, S.B. Lee, J.B. Kim, S.K. Lee, Surf. Coat. Technol. 204 (2010) 1419–1425.
[16] Z.B. Li, B. Shen, Y.D. Deng, L. Liu, W.B. Hu, Appl. Surf. Sci. 255 (2009) 4542–4546.
[17] W. Zhao, Q.Y. Zhang, H.P. Zhang, J.P. Zhang, J. Alloys Compd. 473 (2009) 206–211.
[18] H. Bi, K.C. Kou, A.E. Rider, K. Ostrikov, H.W. Wu, Z.C. Wang, Appl. Surf. Sci. 255 (2009) 6888–6893.
[19] W. Zhao, Q.Y. Zhang, J.P. Zhang, J.W. Gu, F.G. Guo, Polym. Compos. 30 (2009) 1098–1105.
[20] R.H. Wang, J.S. Jiang, M. Hu, Mater. Res. Bull. 44 (2009) 1468–1473.
[21] X.F. Pan, G.H. Mu, N. Chen, K.K. Gan, K. Yang, M.Y. Gu, Mater. Sci. Technol. 23 (2007) 723–726.
[22] X.H. Liu, W.Y. Shih, W.H. Shih, J. Am. Ceram. Soc. 80 (1997) 2781–2788.
[23] K. Ishikawa, T. Uemori, Phys. Rev. B 60 (1999) 11841–11845.
[24] X.A. Li, X.J. Han, P. Xu, Appl. Surf. Sci. 255 (2009) 6125–6131.
[25] M.P. McNeal, S.J. Jang, R.E. Newnham, J. Appl. Phys. 83 (1998) 3288–3297.
[26] K.S. Deepa, S. Kumari Nisha, P. Parameswaran, M.T. Sebastian, J. James, Appl. Phys. Lett. 94 (2009) 142902.
[27] A. Lshimaru, Electromagnetic Wave Propagation, Radiation, and Scattering, Prentice Hall, New Jersey, 1991, p. 17.
[28] Y. Yang, B.S. Zhang, W.D. Xu, Y.B. Shi, N.S. Zhou, H.X. Lu, J. Magn. Magn. Mater. 265 (2003) 119–122.
[29] A. Aharoni, J. Appl. Phys. 69 (1991) 7761–7764.
[30] R. Ramprasad, P. Zurcher, M. Petras, M. Miller, P. Renaud, J. Appl. Phys. 96 (2004) 519–529.